

β -Phorbol ester-induced enhancement of exocytosis in large mossy fiber boutons of mouse hippocampus

Takuya Hikima · Rikita Araki · Toru Ishizuka · Hiromu Yawo

Received: 22 December 2008 / Accepted: 10 February 2009 / Published online: 20 March 2009
© The Physiological Society of Japan and Springer 2009

Abstract β -Phorbol esters (BPE), synthetic analogues of diacylglycerol (DAG), induce the potentiation of transmission in many kinds of synapses through activating the C_1 domain-containing receptors. However, their effects on synaptic vesicle exocytosis have not yet been investigated. Here, we evaluated the vesicular exocytosis directly from individual large mossy fiber boutons (LMFBs) in hippocampal slices from transgenic mice that selectively express synaptopHluorin (SpH). We found that the activity-dependent increment of SpH fluorescence (ΔSpH) was enhanced by 4 β -phorbol 12,13-diacetate (PDAC), one of the BPEs, without influencing the recycled component of SpH. These PDAC effects on ΔSpH were almost completely inhibited by staurosporine, a non-selective antagonist of protein kinases. However, intermittent synaptic transmission was still potentiated through a staurosporine-resistant mechanism. The staurosporine-sensitive cascade may facilitate the vesicle replenishment, thus maintaining the fidelity of transmission at a high level during repetitive firing of the presynaptic neuron.

Keywords Exocytosis · Synaptic transmission · Presynaptic mechanism · PKC · Munc13-1 · Synaptic plasticity

Introduction

In the central nervous system (CNS) signals are transmitted from neuron to neuron at synapses. Synapses are also the principal sites of short- and long-term changes of neuronal networks. In the hippocampus, the axon of a dentate granule cell (mossy fiber, MF) provides robust excitatory inputs on 11–18 CA3 pyramidal cells at their proximal dendrites [1, 2]. Each transmission is mediated by a large MF bouton (LMFB), which forms a complex of tens of excitatory synapses. The MF-CA3 transmission is also highly dynamic over a large range during short- and long-term plasticity. These peculiar morphological and physiological features led to the proposal that the MF input might be involved in filtering out context for building the complete episodic memory [3]. Pharmacological studies using β -phorbol esters (BPE), synthetic analogues of diacylglycerol (DAG), one of the signaling messengers produced by phospholipases, showed that they induced the potentiation of transmission in many kinds of synapses through activating the C_1 domain-containing receptors [4, 5]. The BPEs are amongst the most potent in up-regulating the transmission at the MF-CA3 synapse, suggesting that the DAG/BPE-dependent cascade is involved in the plasticity of this synapse [6–10]. However, their effects on synaptic vesicle exocytosis have not yet been investigated.

The inside of a secretory vesicle is acidic (pH 5.6), whereas it becomes neutral (pH 7.4) instantaneously upon exocytosis [11]. The intravesicular change of pH is optically detected by a fluorescence change of a pH-sensitive

Electronic supplementary material The online version of this article (doi:10.1007/s12576-009-0031-0) contains supplementary material, which is available to authorized users.

T. Hikima · R. Araki · T. Ishizuka · H. Yawo (✉)
Department of Developmental Biology and Neuroscience,
Tohoku University Graduate School of Life Sciences,
2-1 Seiryomachi, Aoba-ku, Sendai 980-8575, Japan
e-mail: yawo@mail.tains.tohoku.ac.jp

T. Hikima · H. Yawo
Tohoku University Basic and Translational Research
Centre for Global Brain Science, Sendai 980-8575, Japan

derivative of green fluorescent protein (pHluorin) when it is expressed inside the secretory vesicles by fusing to the luminal domain of a vSNARE-type vesicular membrane protein synaptobrevin/VAMP-2 [11–13]. In this paper we optically evaluated the exocytosis-dependent changes of fluorescence from individual LMFs in acute hippocampal slices from transgenic mice that express this fusion protein (synaptopHluorin, SpH) only in the MF boutons [14]. We found that one of the BPEs, 4 β -phorbol 12,13-diacetate (PDAc) enhanced the activity-dependent SpH response in a single LMF without influencing the SpH recycling rate. This effect of PDAc was almost completely blocked by staurosporine, which inhibits a broad spectrum of protein kinases at their ATP-binding sites, but not the non-PKC C₁ domain-containing receptors. It is suggested that BPEs enhance the activity-dependent exocytosis of synaptic vesicles through mechanisms involving protein kinases.

Methods

Hippocampal slice preparation

The experiments were carried out using 14–21-day-old heterozygous mice from one of the thy-1 promoter-synaptopHluorin (SpH) transgenic lines with the background of C57BL/6, TV-42, RIKEN BRC, acc. no. 01519 (<http://www.brc.riken.jp/lab/animal/en/>), which express SpH selectively in the mossy fiber (MF) boutons of the hippocampus [14]. The mice were decapitated under ether-anesthesia, and hippocampal slices (300–400 μ m) were prepared as described [15]. For the dissection, a cutting solution containing (in mM) 229 mannitol, 3 KCl, 26 NaHCO₃, 1 H₃PO₄, 7 MgCl₂, 0.2 lidocaine HCl, pH 7.4 (0°C) with 95% O₂ and 5% CO₂ mixed gas was used. Experiments were done at 23–25°C, while the slices were superfused (2 ml/min) with artificial cerebrospinal fluid (ACSF) containing (in mM) 114 NaCl, 2.5 KCl, 26 NaHCO₃, 1 NaH₂PO₄, 10 mannitol, 2.5 CaCl₂, 1.3 MgCl₂, 10 glucose (pH 7.4 with 95% O₂ and 5% CO₂ mixed gas). All animal procedures were conducted in accordance with the guiding principles of the Physiological Society of Japan and NIH.

Extracellular recordings

Field excitatory postsynaptic potentials (fEPSPs) were recorded in the stratum lucidum of the CA3 region using glass microelectrodes with a pipette resistance of 0.7–2 M Ω filled with 1.75% Na₂SO₄ solution. A tungsten bipolar stimulating electrode was placed in the dentate hilus, and two electrical pulses (200 μ s duration, 150–250 μ A intensity, 100 ms inter-stimulus interval) were

delivered intermittently every 30 s. At the end of the experiments, we examined the sensitivity of fEPSP to either 1 μ M DCG-IV or 10 μ M L-CCG-1, an agonist for the group-II metabotropic glutamate receptors, which are selectively expressed in the MF presynaptic terminals [16, 17]. Although the MF synaptic transmission is only slightly attenuated by these drugs after β -phorbol ester-induced potentiation [18], a reduction of fEPSPs was actually observed in the range of 10–60%. Recordings were made with a Gene Clamp amplifier (Axon Instruments, Foster City, CA) and amplified and filtered at 10 kHz with an FLA-01 amplifier (Cygnus Technology, Inc., Delaware Water Gap, PA), digitized at 20 kHz with a DigiData 1320 A/D converter (Axon Instruments). Data were analyzed with Clampfit 9.2 software (Axon Instruments).

Optical imaging of exocytosis

SpH was excited with an argon laser at 488 nm, and fluorescence was collected through a 505-nm long-pass filter under conventional confocal microscopy equipped with a 63 \times 0.95 NA objective (LSM 510 META, Carl Zeiss, Oberkochen, Germany). Individual MF boutons were identified in the stratum lucidum of acute slices of hippocampus by SpH fluorescence (Fig. 1a, b) as some SpH molecules are distributed in the plasma membrane [13, 14, 19]. Throughout every experiment the fluorescence intensity of a region of interest (ROI) was measured with fixed sensitivity and was expressed in arbitrary fluorescence units (AFU), while the laser power was also set at a fixed intensity. The sampling frequency of images was set at 2 Hz (Figs. 1, 2, 3, 4c, and 5) or 1 Hz (Fig. 4a). Since only a small subset of LMFs was responsive to the MF stimulation, they were detected by the following protocol. The LMFs were electrically stimulated at 10 Hz for 10 s, while confocal images (512 \times 512 pixels) were sampled (Fig. 1c, d). To identify the LMFs, three bright fluorescent spots in the same focal plane were used as landmarks. Once one of the landmarks went out of focus, the experiment was no longer included in the analysis. Both baseline and responsive images were median-filtered at 5 pixels, and the difference image was calculated by subtracting the baseline image from the response image (Supplementary movie). Subsequently, the difference image was median-filtered at 8 pixels, and the signals derived from small-sized boutons or non-specific intrinsic fluorescence was largely removed. Each spot with brightness greater than a threshold of 10 AFU was defined as a responsive LMF (Fig. 1e). Circular ROIs of 2.24- μ m diameter were set at the responsive LMFs, and the time series data of ROIs were acquired from raw image stacks. At least ten other ROIs were also set at non-responsive MF regions of the same image, and the background fluorescence changes were recorded. The background fluorescence changes, which

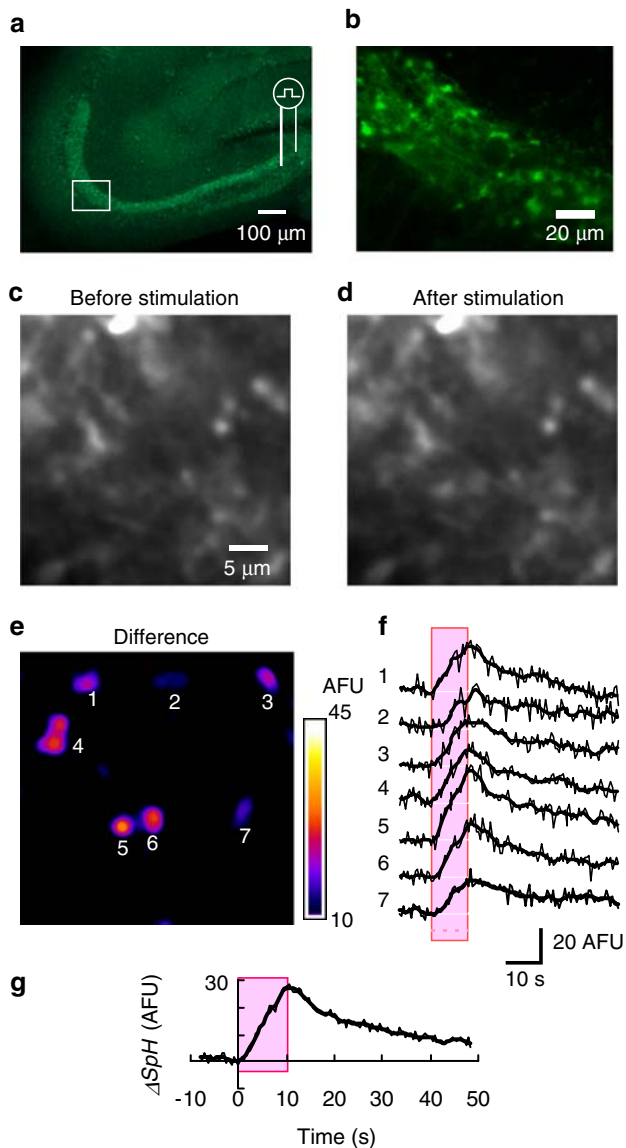


Fig. 1 Synaptic vesicle dynamics in individual large MF boutons (LMFBs) in the hippocampus. **a** A synaptotfluorin (SpH) fluorescence image of an acute slice of TV-42 transgenic mouse hippocampus. The MFs were stimulated at the dentate hilus (*right*) and recorded from the distal CA3 region (*left square*). **b** An enlarged view of the stratum lucidum included in the square in **a**. Individual LMFBs are identifiable by the SpH fluorescence in the plasma membrane. **c** A sample averaged image of the SpH fluorescence of LMFBs before nerve stimulation. **d** Similar to **c**, but the images were sampled near the end of repetitive stimulation of 10 Hz for 10 s. **e** The digital subtraction of both images (difference image). The magnitude is shown as a pseudocolor rating. **f** Time-dependent profiles of SpH fluorescence signals of the ROIs indicated in **e**. The stimulation period is indicated by a red stripe. **g** Average SpH signal profile of sample records in **f**. Note that the fluorescence intensity steadily increased during repetitive stimulation, but recovered to the baseline after the cessation of stimulation

were mainly derived from the fluorescence bleaching, were averaged, normalized to the value at time 0 (the normalized background fluorescence). For each ROI the effect of

fluorescence bleaching was removed by dividing the SpH fluorescence value by the normalized background fluorescence value of the same time point. The time-dependent change of the SpH fluorescence intensity was thus obtained for each ROI (Fig. 1f, thin lines). These ratio data were also digitally filtered by applying a weighted moving-average protocol as described [15] (Fig. 1f, thick lines). The weights, 0.080251, 0.137137, 0.182615, 0.2, 0.182615, 0.137137 and 0.080251, were designed by the Kaiser window finite impulse response (FIR) algorithm so that the sum of the squares of errors was minimized, while the sum of the weights was equal to 1. The mean noise amplitude was calculated as the average of the absolute difference between the raw ratio data and the filtered ratio data. The signal range was calculated by subtracting the minimal filtered ratio value during another 10 s just before stimulation from the maximal filtered ratio value during 10-s repetitive stimulation. The signal-to-noise ratio (S/N) was thus obtained by dividing this signal range by the mean noise amplitude. If S/N < 5, the data were not employed for the subsequent analyses. The time-dependent change of the ratio data (ΔSpH) was obtained by subtracting the minimal filtered ratio value from the ratio data. In the following figures showing the ΔSpH , the thin lines represent ratio data before filtering and the thick lines those after filtering. Averaged ΔSpH are also shown as in Fig. 1g. Image analysis was performed with ImageJ software (<http://rsb.info.nih.gov/ij/>), and the time series data of ROIs were sampled in digits and analyzed with Excel software (Microsoft, USA) and R software (<http://cran.r-project.org/>).

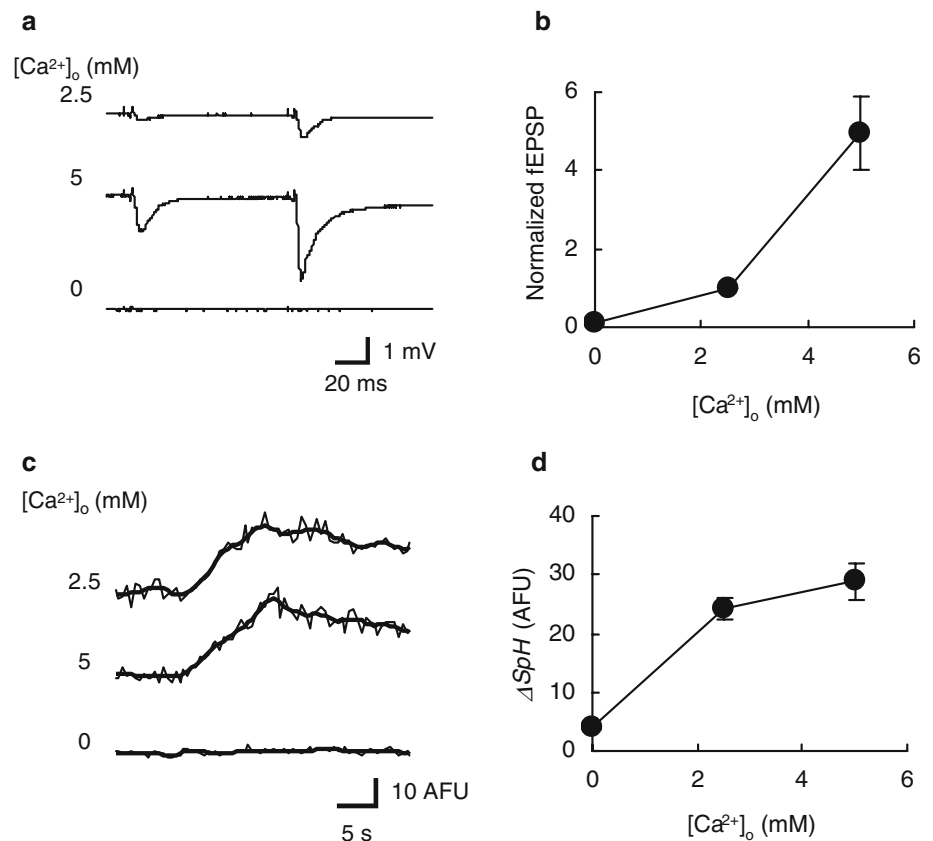
Chemicals

Pharmacological reagents were bath-applied in the recording chamber (2 ml) at a constant flow rate (2 ml/min). Reagents used in this study and their sources were as follows: kynurenic acid (Sigma-Aldrich, St. Louis, MO), lidocaine HCl (Sigma-Aldrich), (2S,2'R,3'R)-2-(2',3'-dicarboxycyclopropyl)glycine (DCG-IV, Tocris Cookson, Bristol, UK); (2S,1'S,2'S)-2-(2-carboxycyclopropyl)glycine (L-CCG-1, Tocris), bafilomycin A1 (Wako, Osaka, Japan); 4 β -phorbol 12,13-diacetate (PDAc, Wako); 4 α -phorbol (Sigma-Aldrich); staurosporine (Sigma-Aldrich). Bafilomycin A1 was dissolved in DMSO containing 20% pluronic acid, then diluted. PDAc, 4 α -phorbol and staurosporine were dissolved in DMSO, then diluted. Stocks of these were preserved at -20°C .

Statistical analysis

Values are expressed as mean \pm SEM (number of experiments) unless otherwise noted. Statistical significance was tested by the Wilcoxon signed-ranks test for paired data

Fig. 2 Ca^{2+} sensitivity of ΔSpH . **a** Sample records of fEPSP evoked by a two-pulse protocol (interval, 100 ms) at 0.033 Hz in an ACSF containing $[\text{Ca}^{2+}]_o$ at 2.5 mM (top trace), 5 mM (middle trace) or 0 mM (bottom trace). **b** $[\text{Ca}^{2+}]_o$ dependence of fEPSP ($n = 8$ slices). **c** Sample records of ΔSpH from a LMFB by a train of repetitive stimulation (10 Hz for 10 s); $[\text{Ca}^{2+}]_o$ at 2.5 mM (top trace), 5 mM (middle trace) or 0 mM (bottom trace). **d** $[\text{Ca}^{2+}]_o$ dependence of ΔSpH ($n = 12$ boutons, 3 slices)



and by the Mann–Whitney U -test or the Kolmogorov–Smirnov test for unpaired data. The significance limit was set at $P = 0.05$ in any test.

Results

Ca^{2+} -sensitivity of ΔSpH

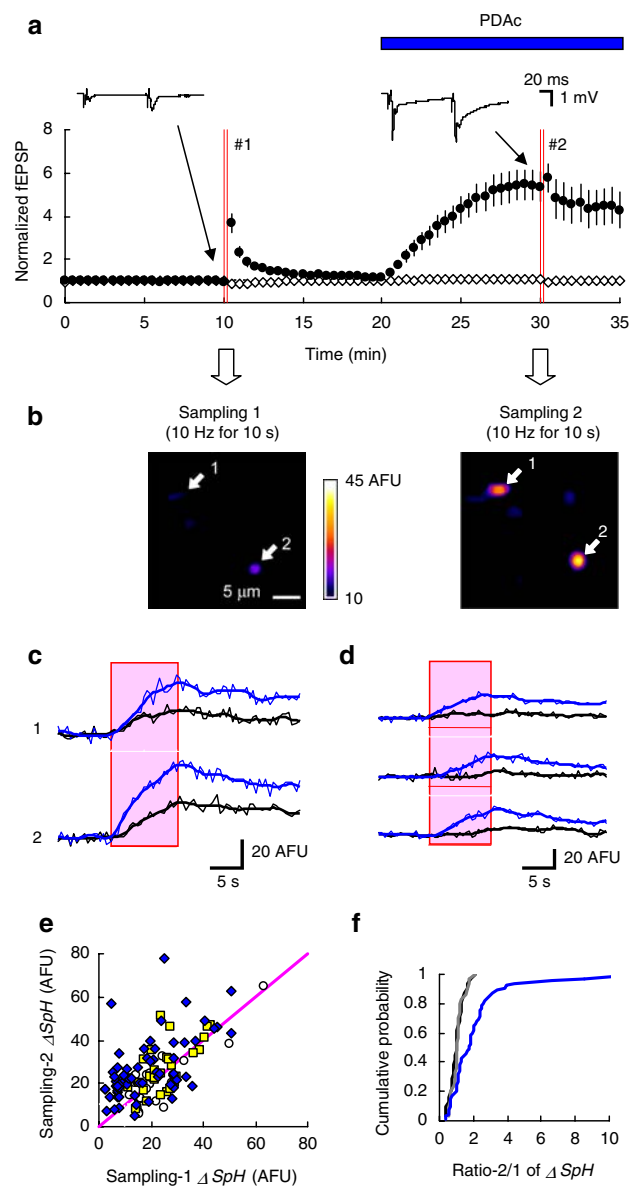
In this study we measured the basal synaptic transmission using the first fEPSPs of paired stimuli at 0.033 Hz. On the other hand, the ΔSpH is the cumulative response to the repetitive stimulation (10 Hz for 10 s). The first fEPSP is dependent on the size of the readily releasable pool (RRP), where the vesicles are docked/primed to the active zone membrane at each synapse [20–22] and the vesicle fusion probability (see Appendix). During repetitive stimulation at 10 Hz, the vesicular exocytosis is in equilibrium with the vesicle replenishment from the reserve subpopulation of vesicle pool [23] because of the relatively small size of RRP [15, 24]. Therefore, the ΔSpH is expected to be more dependent on the vesicle replenishment than the RRP. To test this, the effects of vesicle fusion probability were investigated by changing $[\text{Ca}^{2+}]_o$. When $[\text{Ca}^{2+}]_o$ was increased from 2.5 mM ($[\text{Mg}^{2+}]_o$, 2.5 mM) to 5 mM ($[\text{Mg}^{2+}]_o$, 0 mM), the fEPSP amplitude was enhanced by

4.94 ± 0.93 -fold ($n = 8$ slices) (Fig. 2a). This enhancement was accompanied with the reduction of paired-pulse ratio from 3.04 ± 0.26 to 2.08 ± 0.11 ($n = 8$ slices). In summary, the fEPSP followed a nonlinear relationship with $[\text{Ca}^{2+}]_o$ (Fig. 2b). On the other hand, the ΔSpH was less sensitive to the same change of $[\text{Ca}^{2+}]_o$ (Fig. 2c). The mean ΔSpH was 22.3 ± 1.3 AFU at 2.5 mM $[\text{Ca}^{2+}]_o$ and 25.8 ± 1.8 AFU at 5 mM $[\text{Ca}^{2+}]_o$ with significant difference ($n = 24$ boutons, 6 slices, $P < 0.05$ Wilcoxon signed-ranks test). Since the ΔSpH was undetectable when $[\text{Ca}^{2+}]_o$ was 0 mM ($[\text{Mg}^{2+}]_o$, 5 mM; EGTA, 1 mM), its relationship to $[\text{Ca}^{2+}]_o$ was different from that of fEPSP in the $[\text{Ca}^{2+}]_o$ sensitivity (Fig. 2d). These results are consistent with the notion that the first fEPSP and the ΔSpH are distinct in their aspects of the exocytosis.

BPE-dependent enhancement of ΔSpH

Previously, it was shown that the fEPSP is augmented by PDAC at the stratum lucidum of the hippocampus at the concentration of 0.5–10 μM [6, 7, 9, 10, 18]. This was also the case in the present study, and the fEPSP was potentiated by 10 μM PDAC to, on average, $533 \pm 64\%$ ($n = 8$ slices) of control (Fig. 3a, filled circles). On the other hand, the PDAC treatment did not affect the amplitude of the fiber volley response preceding the fEPSP, which is an indication

Fig. 3 Enhancement of the activity-dependent increment of SpH fluorescence (ΔSpH) by β -phorbol esters (BPE). **a** The fEPSP was monitored at 0.033 Hz using a two-pulse protocol (insets left, before and right, after PDAc); the peak amplitude of the first fEPSP (filled circles, mean \pm SEM, $n = 8$ slices) and the fiber volley amplitude (open diamonds, mean \pm SEM, $n = 3$ slices). Each data was normalized to the mean of five values preceding the sampling 1. The numbered red double lines indicate image sampling 1 and 2 when repetitive stimulations were applied at 10 Hz for 10 s. Drugs were bath-applied for the indicated periods. **b** The difference images of the same region before (left, sampling 1) and after PDAc (10 μ M) (right, sampling 2). **c** The sample ΔSpH traces during MF stimulation of three LMFBs in **b** (indicated by white arrows) are compared before (sampling 1, black) and after PDAc (sampling 2, blue). **d** In some LMFBs, the negligibly small ΔSpH before (sampling 1, black) became obvious after PDAc (sampling 2, blue). **e** Each LMFB was plotted two-dimensionally to the sampling-1 (control) and the sampling-2 (test) values of ΔSpH ; vehicle alone (open circles, $n = 31$ boutons, 5 slices), 4 α -phorbol (yellow squares, $n = 30$ boutons, 6 slices) and PDAc (blue diamonds, $n = 65$ boutons, 10 slices). The magenta line shows that both are equal. **f** Cumulative probability plots of the ratio value of the ΔSpH at sampling 2 divided by that at sampling 1 (ratio-2/1 of ΔSpH); vehicle alone (black line), 4 α -phorbol (gray line) and PDAc (blue line)



of the number of stimulated axons (open diamonds, mean $110 \pm 4\%$, $n = 3$ slices). As shown in the Fig. 3a insets, the PDAc treatment significantly reduced the paired-pulse ratio from 2.1 ± 0.14 to 1.2 ± 0.03 ($n = 8$ slices, $P < 0.01$, Wilcoxon signed-ranks test), suggesting the involvement of presynaptic mechanisms [10]. The SpH images were sampled twice before (Fig. 3a, red double line no. 1) and after PDAc treatment (red double line no. 2). Figure 3b shows representative ΔSpH images (10 Hz for 10 s) before (left, sampling 1) and after (right, sampling 2) the treatment with PDAc. The PDAc treatment obviously enhanced the ΔSpH in some LMFBs (white arrows) as shown in the sample records in Fig. 3c. The effects of PDAc on the individual MF boutons were variable from bouton to bouton, and the boutons that responded to the repetitive stimulation with negligibly small ΔSpH often became obvious after PDAc (Fig. 3d). Figure 3e summarizes the effects of PDAc in which the ΔSpH values at sampling 2 were plotted to those at sampling 1 (blue diamonds, $n = 65$ boutons, 10 slices). The maximal ΔSpH at the end of a train of stimulation was 18.3 ± 1.5 AFU at sampling 1 and 26.5 ± 1.7 AFU at sampling 2, and the difference was significant ($P < 0.0001$, Wilcoxon signed-ranks test). We also plotted in the same figure the effects of the vehicle (DMSO) alone (white circles, $n = 31$ boutons, 5 slices, 22.0 ± 2.0 AFU at sampling 1 and 21.2 ± 1.9 AFU at sampling 2) and those of 4 α -phorbol (10 μ M), one of the inactive phorbol esters (yellow square, $n = 30$ boutons, 6 slices, 25.5 ± 1.5 AFU at sampling 1 and 27.1 ± 2.0 AFU at sampling 2). The ΔSpH at sampling 2 was virtually unchanged from that at sampling 1 by these control treatments. The effects of PDAc were more clearly shown by

comparing the ratio value of the ΔSpH at sampling 2 divided by that at sampling 1 (ratio-2/1 of ΔSpH) in cumulative probability plots (Fig. 3f). Although the PDAc significantly enhanced the ΔSpH ($P < 0.0005$, Kolmogorov–Smirnov test), the effects of 4 α -phorbol were indistinguishable from the vehicle alone control. This is consistent with the notion that the 4 α -phorbol esters are biologically inactive [4] and that the PDAc-dependent enhancement of the ΔSpH appeared to be specific to the C₁ domain-containing receptors such as PKC and Munc13s [4, 5, 25].

Evaluation of SpH recycling

After fusion, the SpH molecules in the vesicular membrane are exposed to the extracellular space (pH 7.4) and

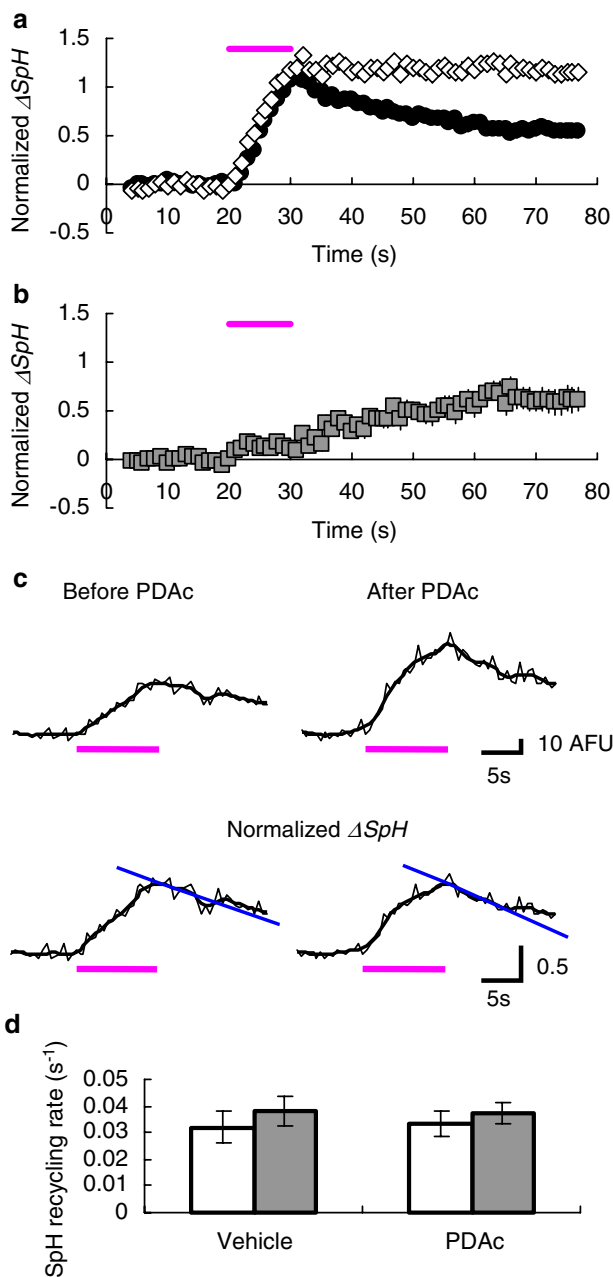


Fig. 4 Effects of BPE on the rate of SpH recycling. **a** The ΔSpH signals were normalized and averaged before (closed circles) and after 5 μM bafilomycin A1 (open diamonds) (mean \pm SEM, $n = 30$ boutons, 7 slices). **b** The contribution of SpH recycling through the processes of endocytosis-reacidification was estimated by the subtraction of the ΔSpH before bafilomycin A1 from that after, and was plotted (gray squares, mean \pm SEM, $n = 30$ boutons, 7 slices). **c** Each ΔSpH signal before (top left) and after PDAc (top right) was normalized to the value at the end of a train of repetitive stimulations (bottom traces) and a regression line (blue) was fitted to the data of 0–5 s after the last stimulation. **d** Summary (mean \pm SEM) of the SpH recycling rate before (open columns) and after vehicle alone (DMSO, left filled column, $n = 27$ boutons, 4 slices) or PDAc (right filled column, $n = 44$ boutons, 10 slices)

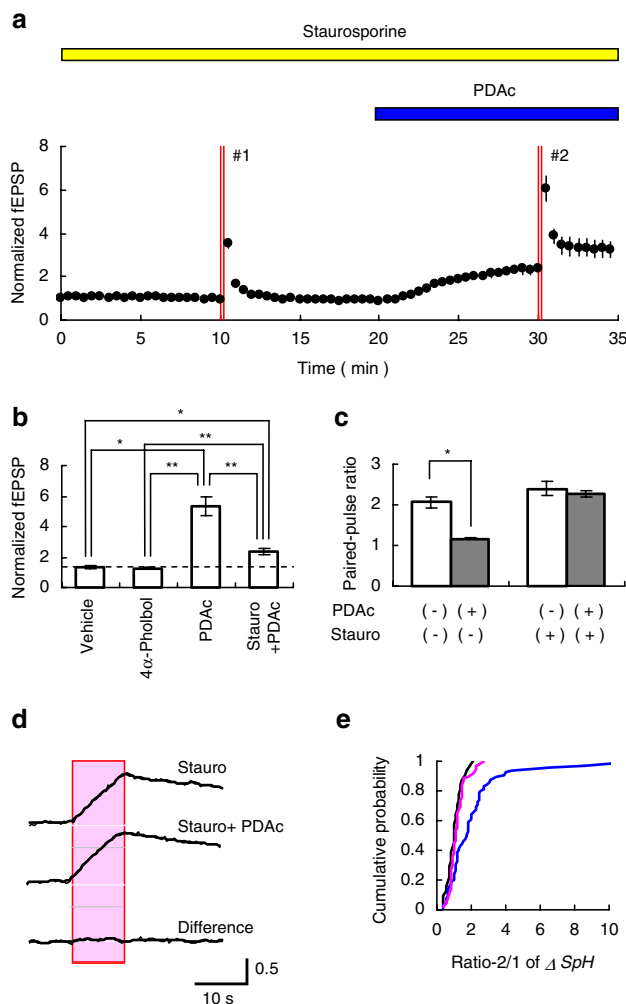


Fig. 5 Effects of staurosporine. **a** The effects of PDAc on fEPSPs in the presence of 1 μM staurosporine. The numbered double lines indicate image sampling 1 and 2. Reagents were bath-applied for the indicated periods. **b** Summary of the effects on the first fEPSP amplitude of the treatments: vehicle alone (first left, $n = 5$ slices), 4 α -phorbol (second left, $n = 7$ slices), PDAc (third left, $n = 8$ slices) and staurosporine plus PDAc (right most, $n = 12$ slices). * $P < 0.01$ and ** $P < 0.0005$ (Mann–Whitney U -test). **c** Summary of the effects of PDAc on the paired-pulse ratio of fEPSPs in the absence (left, $n = 8$ slices) and the presence of staurosporine (right, $n = 12$ slices). Open column, paired-pulse ratio before PDAc treatment; closed column, 10 minutes after exposure to PDAc. * $P < 0.01$ (Wilcoxon signed-ranks test). **d** Average fluorescence profiles of LMFBs ($n = 65$ boutons, 15 slices) in the presence of staurosporine before (top), after PDAc (middle) and the difference (bottom). **e** Cumulative probability plots of the ratio-2/1 value of ΔSpH ; vehicle alone (black line), PDAc (blue line) and staurosporine plus PDAc (magenta line)

de-protonated to become fluorescent [11–13]. The synaptic vesicles are then recycled into a vesicular pool, refilled with transmitter and reutilized for the following transmission [22, 26]. The SpH molecules are retrieved from the

plasma membrane with the new vesicles during the process of endocytosis and are protonated to become non-fluorescent with the progress of the reacidification of the intravesicular space by the activity of V-type H⁺ ATPase [19, 27]. Therefore, the rising phase of the ΔSpH represents the difference between the exocytosis and the molecule's recycling through the process of endocytosis-reacidification, whereas the falling phase kinetics are solely dependent on the recycling [15, 27, 28]. The PDAC can enhance the ΔSpH either through increasing the exocytosis rate or through decreasing the recycling rate.

When the intravesicular reacidification is completely blocked by bafilomycin A1, a potent inhibitor of the V-type H⁺ ATPase [13, 15], the recycling vesicles are expected to be trapped in alkaline. To evaluate the contribution of the recycled SpH, the ΔSpH was normalized to the value at the end of the train stimulation (10 Hz for 10 s) in the absence of bafilomycin A1, and the effects of bafilomycin A1 were examined as shown in Fig. 4a. As expected the falling rate of the SpH response was almost null in the presence of 5 μ M bafilomycin A1. Therefore, the contribution of recycled SpH was estimated by subtraction of the ΔSpH before bafilomycin A1 from that after (Fig. 4b). This bafilomycin A1-sensitive component steadily increased during the train stimulation, and was $10 \pm 6\%$ ($n = 30$ boutons, 7 slices) at the end of the train stimulation. The bafilomycin A1-sensitive component was again examined in the presence of PDAC, was $16 \pm 8\%$ ($n = 26$ boutons, 3 slices), and was insignificantly different from the value in the absence ($P > 0.5$, Mann–Whitney *U*-test).

The recycling rate of SpH during the train stimulation can also be approximated by the initial rate of the fluorescence reduction after the last stimulation (Fig. 4b) [28]. As the first step, the filtered ΔSpH was normalized to the value at the end of the train stimulation (10 Hz for 10 s). Next, a regression line was fitted to the data of 0–5 s after the last stimulation, and its slope was adopted as the SpH recycling rate (Fig. 4c). As shown in Fig. 4d, the effects of PDAC on the SpH recycling rate were almost negligible and were similar to the effects of vehicle alone ($P > 0.5$, Mann–Whitney *U*-test).

Taken together, there was no evidence that PDAC decreased the SpH recycling rate. The PDAC-dependent enhancement of the SpH response is well attributable to the change of the exocytosis rate.

Effects of staurosporine

Since the SpH response was specifically enhanced by PDAC, but not by 4 α -phorbol, the PDAC-dependent enhancement of the SpH response appeared to be specific to the C₁ domain-containing receptors such as PKC and Munc13s [4, 5, 25]. To investigate the downstream

mechanisms of BPE, we examined the effects of staurosporine, which inhibits a broad spectrum of protein kinases at their ATP-binding sites [29, 30]. As shown in Fig. 5a, the PDAC potentiated the fEPSP to a mean $232 \pm 20\%$ ($n = 12$ slices) of control in the presence of staurosporine (1 μ M). Although the magnitude of this potentiation was significantly smaller than in the absence of staurosporine ($P < 0.0001$, Mann–Whitney *U*-test), it was still significantly greater than the control (vehicle alone and 4 α -phorbol treatments, $P < 0.01$, Mann–Whitney *U*-test) (Fig. 5b). During the PDAC-induced fEPSP potentiation, the paired-pulse ratio was always decreased from its initial value. However, this was not the case in the presence of staurosporine (Fig. 5c), and the paired-pulse ratio was on average 2.3 ± 0.09 ($n = 12$ slices), which is insignificantly different from the control (2.4 ± 0.17 , Wilcoxon signed-ranks test).

As shown in Fig. 5d, the average profiles of the ΔSpH ($n = 65$ boutons, 15 slices) were compared before and after PDAC (10 μ M), while the slices were pretreated with staurosporine (1 μ M). The maximal ΔSpH at the end of a train of stimulation was 26.7 ± 1.3 AFU at sampling 1 and 26.4 ± 1.4 AFU at sampling 2, and the difference was insignificant ($P > 0.7$, Wilcoxon signed-ranks test). The subtracted curve (difference) indicates that PDAC was almost ineffective on the ΔSpH in the presence of staurosporine. Figure 5e shows the cumulative probability plots of the ratio-2/1 values of ΔSpH . The effects of PDAC were almost completely blocked by staurosporine ($P < 0.0001$, Kolmogorov–Smirnov test) and indistinguishable from the vehicle alone control. The staurosporine-sensitive cascade appears to be one of the major downstream reactions of PDAC in the case of exocytosis during repetitive activation of the LMFBS. This is in contrast to the case of intermittent synaptic transmission (e.g., 0.033 Hz) where a significant potentiation remained even in the presence of staurosporine.

Discussion

The BPEs, such as 4 β -phorbol-12,13-dibutyrate (PDBu, 10 μ M) and PDAC (2 μ M), increased the MF-dependent population spike with negligible effects on the glutamate sensitivity [6]. The PDAC increased the quantum content with little changes in the quantum size [7], and its potentiation was accompanied by a reduction of the paired-pulse ratio [10]. In the present study the PDAC-dependent enhancement of fEPSP was not accompanied by an enhancement of the fiber volley response as previously noted [18], suggesting the up-regulation of synaptic transmission. These lines of electrophysiological evidence suggest that the BPEs would enhance the quantal

transmitter release from the LMFBs. However, the validity of this interpretation has to be re-investigated taking into consideration the nonuniform probability of release, the concentration of glutamate in the synaptic cleft, the effects of the rapid desensitization of the glutamate AMPA receptors and the unsilencing of postsynaptic responsiveness [31–36]. This paper presents additional evidence in a more direct way that the BPEs enhance the exocytosis in a single LMFB in acute hippocampal slices using the SpH transgenic mice. The ΔSpH was enhanced on average 2.2-fold by the PDAC (10 μ M), although the magnitude of potentiation was variable from bouton to bouton. On the other hand, its effect on the recycled component of ΔSpH , which is regulated by the endocytosis and the subsequent reacidification of the vesicles, was negligible. Therefore, the PDAC-dependent change of the ΔSpH could be attributed to the change of the exocytosis rate. However, its effects on the endocytosis have to be further investigated since the synaptobrevin/VAMP-2, which can be detected by the SpH fluorescence, was retrieved from the plasma membrane in a way kinetically differentiated from other vesicle marker proteins, such as the synaptophysin and the vesicular glutamate transporters [37, 38].

It should be noted that our ΔSpH measurement evaluated a different aspect of exocytosis from the previous electrophysiological measurements of synaptic transmission. Since the ΔSpH showed small sensitivity to $[Ca^{2+}]_o$ between 2.5 and 5 mM, the contribution of the vesicle fusion probability is small. Rather, it could be dependent on the magnitude of the vesicle replenishment [15]. However, in the CA3-CA1 synapses of hippocampus, the SpH fluorescence change evoked by a train of repetitive stimulation (10 Hz for 5 s) is dependent on $[Ca^{2+}]_o$ (0.5–5 mM) like fEPSP [39]. It is possible that these two synapses are different in the $[Ca^{2+}]_o$ - ΔSpH relationship, but the underlying mechanisms of this difference should be investigated in future.

Staurosporine-sensitive and -resistant mechanisms

DAG is a key messenger regulating the efficacy of synaptic transmission. The effects of DAG and its analogues, BPEs, are partly mediated by the activation of protein kinase C (PKC), which facilitates exocytosis in a wide variety of cells and presynaptic terminals [40–42]. They also regulate the efficacy of synaptic transmission through activating non-PKC C_1 domain-containing receptor proteins, such as Munc13s, which are presynaptic vesicle priming proteins [43–45]. It has been suggested that the PKC-dependent and Munc13-1-dependent pathways synergistically modulate the exocytosis [4, 5]. In this study the PDAC-dependent enhancement of the ΔSpH was almost completely blocked by staurosporine, one of the broad spectrum protein kinase

inhibitors. This suggests the involvement of some protein kinases in a cascade downstream of the C_1 domain-containing receptors. However, the effects of more specific inhibitors have to be studied to identify the key molecules. A previous study described that the PDAC-induced potentiation of MF synaptic transmission is partially antagonized by a PKC-selective inhibitor, bisindolylmaleimide I (BIS-I), but a BIS-I resistant component of potentiation remained [10]. However, we found that BIS-I and its derivatives, which differentiate PKC from other kinases, were strongly fluorescent at the SpH emission spectra when included in the cell. Therefore, it will be necessary in the future to study the possible involvement of PKC using mice in which one of PKC isoforms is knocked out [46] or RNAi-dependent knockdown of one of the PKC isoforms [47].

We also found that the basal synaptic transmission (e.g., 0.033 Hz) was still potentiated in the presence of staurosporine, whereas the effects on the ΔSpH , which is induced by a train of repetitive stimulation, were completely inhibited. Therefore, during a train of repetitive stimulation of LMFB, the response to the first stimulation, which is detectable by fEPSP, and the integrated exocytosis measured by the ΔSpH would be different in the sensitivity to staurosporine. The effects of staurosporine were almost quantitatively equivalent to those of BIS-I in the case of fEPSP. The PDAC (10 μ M) treatment potentiated the fEPSP to $232 \pm 20\%$ of control in the presence of staurosporine, but to $533 \pm 64\%$ of control in the absence. The same treatment potentiated the fEPSP to $258 \pm 34\%$ in the presence of BIS-I [10]. Since the staurosporine-resistant component of potentiation was not accompanied by a reduction of the paired-pulse ratio, an indication of increased vesicle fusion probability (see Appendix), other mechanisms are suggested to be involved. The possibility should be investigated that the staurosporine-resistant fEPSP potentiation is accompanied by the enhancement of postsynaptic sensitivity to glutamate. The spatio-temporal changes of glutamate concentration are also under the regulation of the amount of transmitter release per vesicle, the speed of glutamate release, the synaptic cleft morphology and the speed of glutamate clearance from the synaptic cleft [48, 49]. The BPEs have been demonstrated to increase the RRP size in other synapses [50–52] as well as in the slow exocytosis of endocrine cells [53], although it remains undetermined whether these effects are actually PKC-dependent or not. Since the RRP is fractionally small in an LMFB [15, 24] and would be depleted in 10–20 action potentials if it is not replenished, its increase would hardly be detectable in our SpH study.

The presence of a staurosporine-resistant component of fEPSP potentiation suggests that the signaling cascade via the non-PKC C_1 domain-containing receptors is involved

in the facilitation of synaptic transmission through these mechanisms. Recently, it has been suggested that Munc13-1, one of the non-PKC C₁ domain-containing receptors, localized to active zones in the presynaptic terminal, may also be involved in the regulation of synaptic efficacy by BPEs [54–56]. When the DAG/BPE-binding site of Munc13-1 is genetically deficient or non-functional, the effects of BPEs are largely impaired [56, 57]. Although the present study did not prove whether BPEs potentiate MF synaptic transmission through Munc13-1, it does not conflict with the notion that the PKC-dependent and Munc13-1-dependent pathways synergistically modulate the exocytosis [4, 5].

The ΔSpH unsilencing

We found that the ΔSpH , which was negligibly small at sampling 1, become obvious at sampling 2 after the PDAC in some LMFBs. These synapses are possibly presynaptically silent or weak in the release ability before PDAC [34]. Alternatively, the transmitter release might be rapidly depressed during repetitive stimulation. These possibilities should be clarified in future studies, e.g., the simultaneous recordings of EPSC and SpH fluorescence. Recent studies using cultured networks of developing hippocampal neurons have described the presence of presynaptically silent synapses, which become transmittable through mechanisms dependent on cAMP-protein kinase A (PKA) or BDNF-Cdc signaling cascades [58–62]. At the CA3-CA1 synapses of the mouse hippocampus, the slow presynaptic component of long-term potentiation (LTP), which is detected by the change of SpH fluorescence, is mediated by the PKA and the L-type Ca²⁺ channels [39]. It is possible that some boutons are unsilenced in the ΔSpH . Since MF-LTP is dependent on the AC-PKA cascade [63, 64], it is probably accompanied with the increased ΔSpH . The unsilencing of ΔSpH might be related to the accumulation and organization of the large arrays of vesicular and non-vesicular molecules required for exocytosis as they are during synaptogenesis [65, 66]. PKC is one of the protein kinases involved in these processes. For example, PKC phosphorylates GAP-43, one of major proteins of the presynaptic and growth cone membrane, during synaptic potentiation [67]. Another PKC substrate is myristoylated alanine-rich C kinase substrate (MARCKS), which is involved in both synaptic maturation and the synaptic plasticity [68, 69].

In the hippocampus of a living animal the signals are usually a train of impulses of variable frequencies [70], sometimes at around 10 Hz (a theta rhythm) [71, 72]. When DAG/BPEs facilitate the fusion probability by increasing the Ca²⁺ influx and the Ca²⁺ sensitivity of exocytosis [10], they up-regulate the transmission efficacy

for impulses arriving early in a train, but down-regulate it for impulses arriving later because of the depletion of RRP. This effect could explain the reduction of the paired-pulse ratio. Even if the RRP were to be increased, the potentiation should be transient if it is not replenished. On the other hand, the staurosporine-sensitive enhancement of exocytosis followed a more prolonged time course. Therefore, the DAG/BPE-dependent signaling cascade is suggested to be involved in the facilitation of the vesicle replenishment through a staurosporine-sensitive mechanism and to maintain the fidelity of transmission at a high level during a train of repetitive firings of the presynaptic neuron.

Acknowledgments We thank S. Sakai for experimental assistance and discussion, Y. Sugiyama and H. Wang for comments on the manuscript, and B. Bell for reading the manuscript. This work was sponsored by Core Research for Evolutional Science and Technology (CREST), Japan Science and Technology Agency (JST) and partly supported by grants-in-aid for scientific research from the Ministry of Education, Culture, Sports, Science and Technology (MEXT) of Japan, Global COE Program (Basic & Translational Research Centre for Global Brain Science), MEXT, Strategic Research Program for Brain Sciences (SRPBS), MEXT, The Naito Foundation and The Novartis Foundation (Japan) for the Promotion of Science.

Appendix

Reduction of the paired-pulse ratio

According to the quantal hypothesis [36, 73], a postsynaptic response (E) is related to the following relationship.

$$E = Npq, \quad (1)$$

where q is the postsynaptic response by a single quantum (quantal size). The meanings of N and p are definition-dependent. If p is regarded as the probability of vesicle fusion to the plasma membrane, then N refers to the number of vesicles drawn from the next action potential, the readily releasable pool (RRP) or the release-ready pool [20–22]. On the other hand, if p is regarded as the release probability of a release site, N should be the number of release sites, the morphological correlates of which are the number of active zones of a presynaptic terminal. When a presynaptic axon is stimulated by two pulses of a short interval, the vesicle fusion probability by the second action potential (p') is generally increased by some mechanisms dependent on the residual Ca²⁺ [74–78]. On the analogy of the Eq. 1, the second postsynaptic response (E') will be expressed as,

$$E' = \{N(1 - p) + R\}p'q'. \quad (2)$$

Here, R is the number of vesicles replenished to the RRP during the interval between the first and the second action potentials, and q' is the quantal size of the second response.

The paired-pulse ratio (r) is thus the function of p with the relationship,

$$r = E'/E = (1 - p + R/N)(p'/p)(q'/q). \quad (3)$$

The value R/N is dependent on the vesicle recycling mechanisms. The value p'/p is dependent on the underlying mechanisms of facilitation. The value q'/q is mainly influenced by the postsynaptic factors, such as the desensitization of transmitter receptors. It is also influenced by the synaptic geometry, such as the narrowness of the synaptic cleft, the transmitter clearance activities, such as the glutamate uptake by the astrocytes as well as the presynaptic factors, such as the transmitter density in the vesicle [48, 49]. Although these values appear to be less variable than p , their effects have to be taken into consideration. Since r is negatively related to p , the enhancement of the vesicle fusion probability at the first action potential (p) is expected to be accompanied with the reduction of r .

References

1. Henze DA, Urban NN, Barrionuevo G (2000) The multifarious hippocampal mossy fiber pathway: a review. *Neuroscience* 98:407–427
2. Nicoll RA, Schmitz D (2005) Synaptic plasticity at hippocampal mossy fibre synapses. *Nat Rev Neurosci* 6:863–876
3. Lisman JE (1999) Relating hippocampal circuitry to function: recall of memory sequences by reciprocal dentate-CA3 interactions. *Neuron* 22:233–242
4. Silinsky EM, Searl TJ (2003) Phorbol esters and neurotransmitter release: more than just protein kinase C? *Br J Pharmacol* 138:1191–1201
5. Brose N, Betz A, Wegmeyer H (2004) Divergent and convergent signaling by the diacylglycerol second messenger pathway in mammals. *Curr Opin Neurobiol* 14:328–340
6. Malenka RC, Madison DV, Nicoll RA (1986) Potentiation of synaptic transmission in the hippocampus by phorbol esters. *Nature* 321:175–177
7. Yamamoto C, Higashima M, Sawada S (1987) Quantal analysis of potentiating action of phorbol ester on synaptic transmission in the hippocampus. *Neurosci Res* 5:28–38
8. Zhang L, Ruehr ML, Dorman RV (1996) Arachidonic acid and oleoylacetyl glycerol induce a synergistic facilitation of Ca^{2+} -dependent glutamate release from hippocampal mossy fiber nerve endings. *J Neurochem* 66:177–185
9. Son H, Carpenter DO (1996) Protein kinase C activation is necessary but not sufficient for induction of long-term potentiation at the synapse of mossy fiber-CA3 in the rat hippocampus. *Neuroscience* 72:1–13
10. Honda I, Kamiya H, Yawo H (2000) Re-evaluation of phorbol ester-induced potentiation of transmitter release from mossy fibre terminals of the mouse hippocampus. *J Physiol* 529:763–776
11. Miesenböck G, De Angelis DA, Rothman JE (1998) Visualizing secretion and synaptic transmission with pH-sensitive green fluorescent proteins. *Nature* 394:192–195
12. Sankaranarayanan S, Ryan TA (2000) Real-time measurements of vesicle-SNARE recycling in synapses of the central nervous system. *Nat Cell Biol* 2:197–204
13. Sankaranarayanan S, De Angelis D, Rothman JE, Ryan TA (2000) The use of pHluorins for optical measurements of presynaptic activity. *Biophys J* 79:2199–2208
14. Araki R, Sakagami H, Yanagawa Y, Hikima T, Ishizuka T, Yawo H (2005) Transgenic mouse lines expressing synaptopHluorin in hippocampus and cerebellar cortex. *Genesis* 42:53–60
15. Suyama S, Hikima T, Sakagami H, Ishizuka T, Yawo H (2007) Synaptic vesicle dynamics in the mossy fiber-CA3 presynaptic terminals of mouse hippocampus. *Neurosci Res* 59:481–490
16. Shigemoto R, Kinoshita A, Wada E, Nomura S, Ohishi H, Takada M, Flor PJ, Neki A, Abe T, Nakanishi S (1997) Differential presynaptic localization of metabotropic glutamate receptor subtypes in the rat hippocampus. *J Neurosci* 17:7503–7522
17. Kamiya H, Ozawa S (1999) Dual mechanism for presynaptic modulation by axonal metabotropic glutamate receptor at the mouse mossy fibre-CA3 synapse. *J Physiol* 518:497–506
18. Kamiya H, Yamamoto C (1997) Phorbol ester and forskolin suppress the presynaptic inhibitory action of group-II metabotropic glutamate receptor at rat hippocampal mossy fibre synapse. *Neuroscience* 80:89–94
19. Gandhi SP, Stevens CF (2003) Three modes of synaptic vesicular recycling revealed by single-vesicle imaging. *Nature* 423:607–613
20. Schikorski T, Stevens CF (1997) Quantitative ultrastructural analysis of hippocampal excitatory synapses. *J Neurosci* 17:5858–5867
21. Schneggenburger R, Meyer AC, Neher E (1999) Released fraction and total size of a pool of immediately available transmitter quanta at a calyx synapse. *Neuron* 23:399–409
22. Rizzoli SO, Betz WJ (2005) Synaptic vesicle pools. *Nat Rev Neurosci* 6:57–69
23. Yawo H (1999) Protein kinase C potentiates transmitter release from the chick ciliary presynaptic terminal by increasing the exocytotic fusion probability. *J Physiol* 515:169–180
24. Rollenhagen A, Sätzler K, Rodríguez EP, Jonas P, Frotscher M, Lübke JHR (2007) Structural determinants of transmission at large hippocampal mossy fiber synapses. *J Neurosci* 27:10434–10444
25. Brose N, Rosenmund C (2002) Move over protein kinase C, you've got company: alternative cellular effectors of diacylglycerol and phorbol esters. *J Cell Sci* 115:4399–4411
26. Heuser JE, Reese TS (1973) Evidence for recycling of synaptic vesicle membrane during transmitter release at the frog neuromuscular junction. *J Cell Biol* 57:315–344
27. Sankaranarayanan S, Ryan TA (2001) Calcium accelerates endocytosis of vSNAREs at hippocampal synapses. *Nat Neurosci* 4:129–136
28. Fernández-Alfonso T, Ryan TA (2004) The kinetics of synaptic vesicle pool depletion at CNS synaptic terminals. *Neuron* 41:943–953
29. Tamaoki T, Nomoto H, Takahashi I, Kato Y, Morimoto M, Tomita F (1986) Staurosporine, a potent inhibitor of phospholipid/ Ca^{++} -dependent protein kinase. *Biochem Biophys Res Commun* 135:397–402
30. Rüegg UT, Burgess GM (1989) Staurosporine, K-252 and UCN-01: potent but nonspecific inhibitors of protein kinases. *Trends Pharmacol Sci* 10:218–220
31. Ozawa S, Kamiya H, Tsuzuki K (1998) Glutamate receptors in the mammalian central nervous system. *Prog Neurobiol* 54:581–618
32. Conti F, Weinberg RJ (1999) Shaping excitation at glutamatergic synapses. *Trends Neurosci* 22:451–458
33. Kullmann DM (2003) Silent synapses: what are they telling us about long-term potentiation? *Philos Trans R Soc Lond B Biol Sci* 358:727–733

34. Voronin LL, Cherbini E (2004) ‘Deaf, mute and whispering’ silent synapses: their role in synaptic plasticity. *J Physiol* 557:3–12
35. Lisman JE, Raghavachari S, Tsien RW (2007) The sequence of events that underlie quantal transmission at central glutamatergic synapses. *Nat Rev Neurosci* 8:597–609
36. Yawo H (2009) Quantal transmission. In: Binder MD, Hirokawa N, Windhorst U (eds) *Encyclopedia of neuroscience*. Springer, Berlin. doi:10.1007/978-3-540-29678-2_2867
37. Granseth B, Odermatt B, Royle SJ, Lagnado L (2006) Clathrin-mediated endocytosis is the dominant mechanism of vesicle retrieval at hippocampal synapses. *Neuron* 51:773–786
38. Voglmaier SM, Kam K, Yang H, Fortin DL, Hua Z, Nicoll RA, Edwards RH (2006) Distinct endocytic pathways control the rate and extent of synaptic vesicle protein recycling. *Neuron* 51:71–84
39. Bayazitov IT, Richardson RJ, Fricke RG, Zakharenko SS (2007) Slow presynaptic and fast postsynaptic components of compound long-term potentiation. *J Neurosci* 27:11510–11521
40. Majewski H, Iannazzo L (1998) Protein kinase C: a physiological mediator of enhanced transmitter output. *Prog Neurobiol* 55:463–475
41. Wierda KDB, Toonen RFG, de Wit H, Brussaard AB, Verhage M (2007) Interdependence of PKC-dependent and PKC-independent pathways for presynaptic plasticity. *Neuron* 54:275–290
42. Korogod N, Lou X, Schneggenburger R (2007) Posttetanic potentiation critically depends on an enhanced Ca^{2+} sensitivity of vesicle fusion mediated by presynaptic PKC. *Proc Natl Acad Sci USA* 104:15923–15928
43. Mochida S, Orita S, Sakaguchi G, Sasaki T, Takai Y (1998) Role of the Doc2a-Munc13-1 interaction in the neurotransmitter release process. *Proc Natl Acad Sci USA* 95:11418–11422
44. Augustin I, Rosenmund C, Südhof TC, Brose N (1999) Munc13-1 is essential for fusion competence of glutamatergic synaptic vesicles. *Nature* 400:457–461
45. Basu J, Betz A, Brose N, Rosenmund C (2007) Munc13-1 C1 domain activation lowers the energy barrier for synaptic vesicle fusion. *J Neurosci* 27:1200–1210
46. Hodge CW, Mehmert KK, Kelley SP, McMahon T, Haywood A, Olive MF, Wang D, Sanchez-Perez AM, Messing RO (1999) Supersensitivity to allosteric GABA_A receptor modulators and alcohol in mice lacking PKC ϵ . *Nat Neurosci* 2:997–1002
47. Park Y-S, Hur E-M, Choi B-H, Kwak E, Jun D-J, Park S-J, Kim K-T (2006) Involvement of protein kinase C- ϵ in activity-dependent potentiation of large dense-core vesicle exocytosis in chromaffin cells. *J Neurosci* 26:8999–9005
48. Liu G (2003) Presynaptic control of quantal size: kinetic mechanisms and implications for synaptic transmission and plasticity. *Curr Opin Neurobiol* 13:324–331
49. Tzingounis AV, Wadiche JI (2007) Glutamate transporters: confining runaway excitation by shaping synaptic transmission. *Nat Rev Neurosci* 8:935–947
50. Stevens CF, Sullivan JM (1998) Regulation of the readily releasable vesicle pool by protein kinase C. *Neuron* 21:885–893
51. Waters J, Smith SJ (2000) Phorbol esters potentiate evoked and spontaneous release by different presynaptic mechanisms. *J Neurosci* 20:7863–7870
52. Virmani T, Ertunc M, Sara Y, Mozhayeva M, Kavalali ET (2005) Phorbol esters target the activity-dependent recycling pool and spare spontaneous vesicle recycling. *J Neurosci* 25:10922–10929
53. Gillis KD, Mossner R, Neher E (1996) Protein kinase C enhances exocytosis from chromaffin cells by increasing the size of the readily releasable pool of secretory granules. *Neuron* 16:1209–1220
54. Betz A, Ashery U, Rickmann M, Augustin I, Neher E, Südhof TC, Rettig J, Brose N (1998) Munc13-1 is a presynaptic phorbol ester receptor that enhances neurotransmitter release. *Neuron* 21:123–136
55. Hori T, Takai Y, Takahashi T (1999) Presynaptic mechanism for phorbol ester-induced synaptic potentiation. *J Neurosci* 19:7262–7267
56. Rhee JS, Betz A, Pyott S, Reim K, Varoqueaux F, Augustin I, Hesse D, Südhof TC, Takahashi M, Rosenmund C, Brose N (2002) β phorbol ester- and diacylglycerol-induced augmentation of transmitter release is mediated by Munc13s and not by PKCs. *Cell* 108:121–133
57. Lou X, Korogod N, Brose N, Schneggenburger R (2008) Phorbol esters modulate spontaneous and Ca^{2+} -evoked transmitter release via acting on both Munc13 and protein kinase C. *J Neurosci* 28:8257–8267
58. Tong G, Malenka RC, Nicoll RA (1996) Long-term potentiation in cultures of single hippocampal granule cells: a presynaptic form of plasticity. *Neuron* 16:1147–1157
59. Ma L, Zalbow L, Kandel ER, Siegelbaum SA (1999) Cyclic AMP induces functional presynaptic boutons in hippocampal CA3-CA1 neuronal cultures. *Nat Neurosci* 2:24–29
60. Gasparini S, Saviane C, Voronin LL, Cherubini E (2000) Silent synapses in the developing hippocampus: lack of functional AMPA receptors or low probability of glutamate release. *Proc Natl Acad Sci USA* 97:9741–9746
61. Kohara K, Ogura A, Akagawa K, Yamaguchi K (2001) Increase in number of functional release sites by cyclic AMP-dependent protein kinase in cultured neurons isolated from hippocampal dentate gyrus. *Neurosci Res* 41:79–88
62. Shen W, Wu B, Zhang Z, Dou Y, Rao ZR, Chen YR, Duan S (2006) Activity-induced rapid synaptic maturation mediated by presynaptic cdc42 signaling. *Neuron* 50:401–414
63. Huang YY, Li XC, Kandel ER (1994) cAMP contributes to mossy fiber LTP by initiating both a covalently mediated early phase and macromolecular synthesis-dependent late phase. *Cell* 79:69–79
64. Villacres EC, Wong ST, Chavkin C, Storm DR (1998) Type I adenylyl cyclase mutant mice have impaired mossy fiber long-term potentiation. *J Neurosci* 18:3186–3194
65. Ziv NE, Garner CC (2004) Cellular and molecular mechanisms of presynaptic assembly. *Nat Rev Neurosci* 5:385–399
66. Zhen M, Jin Y (2004) Presynaptic terminal differentiation: transport and assembly. *Curr Opin Neurobiol* 14:280–287
67. Schaechter JD, Benowitz LI (1993) Activation of protein kinase C by arachidonic acid selectively enhances the phosphorylation of GAP-43 in nerve terminal membranes. *J Neurosci* 13:4361–4371
68. McNamara RK, Stumpo DJ, Morel LM, Lewis MH, Wakeland EK, Blackshear PJ, Lenox RH (1998) Effect of reduced myristoylated alanine-rich C kinase substrate expression on hippocampal mossy fiber development and spatial learning in mutant mice: transgenic rescue and interactions with gene background. *Proc Natl Acad Sci USA* 95:14517–14522
69. Hama H, Hara C, Yamaguchi K, Miyawaki A (2004) PKC signaling mediates global enhancement of excitatory synaptogenesis in neurons triggered by local contact with astrocytes. *Neuron* 41:405–415
70. Henze DA, Wittner L, Buzsáki G (2002) Single granule cells reliably discharge targets in the hippocampal CA3 network in vivo. *Nat Neurosci* 5:790–795
71. Skaggs WE, McNaughton BL, Wilson MA, Barnes CA (1996) Theta phase precession in hippocampal neuronal populations and the compression of temporal sequences. *Hippocampus* 6:149–172
72. Bland BH, Konopacki J, Dyck RH (2002) Relationship between membrane potential oscillations and rhythmic discharges in identified hippocampal theta-related cells. *J Neurophysiol* 88:3046–3066

73. del Castillo J, Katz B (1954) Quantal components of the end-plate potential. *J Physiol* 124:560–573
74. Zucker RS, Regehr WG (2002) Short-term synaptic plasticity. *Annu Rev Physiol* 64:355–405
75. von Gersdorff H, Borst JG (2002) Short-term plasticity at the calyx of Held. *Nat Rev Neurosci* 3:53–64
76. Felmy F, Neher E, Schneggenburger R (2003) Probing the intracellular calcium sensitivity of transmitter release during synaptic facilitation. *Neuron* 37:801–811
77. Mochida S, Few AP, Scheuer T, Catterall WA (2008) Regulation of presynaptic $\text{Ca}_v2.1$ channels by Ca^{2+} sensor proteins mediates short-term synaptic plasticity. *Neuron* 57:210–216
78. Müller M, Felmy F, Schneggenburger R (2008) A limited contribution of Ca^{2+} current facilitation to paired-pulse facilitation of transmitter release at the rat calyx of Held. *J Physiol* 586:5503–5520